

## Anomalous Large Critical Regions in Power-Law Random Matrix Ensembles

E. Cuevas, V. Gasparian,\* and M. Ortuño

*Departamento de Física, Universidad de Murcia, E-30071 Murcia, Spain*

(Received 27 November 2000; published 11 July 2001)

We investigate numerically the power-law random matrix ensembles. Wave functions are fractal up to a characteristic length whose logarithm diverges asymmetrically with different exponents, 1 in the localized phase and 0.5 in the extended phase. The characteristic length is so anomalously large that for macroscopic samples there exists a finite critical region, in which this length is larger than the system size. The Green's functions decrease with distance as a power law with an exponent related to the correlation dimension.

DOI: 10.1103/PhysRevLett.87.056601

PACS numbers: 72.15.Rn, 71.30.+h, 05.45.Df

The power-law random banded matrix (PRBM) model was introduced by Mirlin *et al.* [1] to describe a 1D sample with random long-range hopping. The model attracted a lot of attention because it can approximately represent a variety of different physical systems: an integrable billiard with a Coulomb scattering center [2], two interacting particles in a 1D random potential [3], quantum chaos in a billiard with a nonanalytic boundary [4], and the Luttinger liquid at finite temperatures [5,6]. As the model describes a whole family of critical theories, it is also interesting for the study of intermediate spectral statistics [7–9].

The model is represented by  $N \times N$  real symmetric matrices whose entries are randomly drawn from a normal distribution with zero mean and a variance depending on the distance of the matrix element from the diagonal,

$$\langle (H_{ij})^2 \rangle = \frac{1}{1 + (|i - j|/b)^{2\alpha}}. \quad (1)$$

From field theoretical considerations [1,5,10,11], the PRBM model was shown to undergo a sharp transition at  $\alpha = 1$  from localized states for  $\alpha > 1$  to delocalized states for  $\alpha < 1$ . This transition is supposed to be similar to an Anderson metal-insulator transition, presenting multifractality of eigenfunctions and nontrivial spectral compressibility at criticality. The parameter  $b$  plays a role analogous to dimensionality establishing the character of the transition.

From a perturbative treatment of the nonlinear  $\sigma$  model and from renormalization group calculations, Mirlin considered different regimes depending on the exponent  $\alpha$ . These models are justified only for  $b \gg 1$ , although the other limiting case can also be studied following Levitov [12]. For  $\alpha \geq 3/2$  the eigenstates are localized, but in contrast to usual tight-binding models they do not decay exponentially, but with a power law with the same exponent  $\alpha$  as the hopping matrix elements [4,13]. For  $1 < \alpha < 3/2$  the states are still localized, but with a different typical length. In both cases, the wave functions are expected to have integrable power-law tails and the dimensionality to be equal to zero. For very large system sizes, the nearest neighbor normalized level spacings  $s$  should be distributed according to the Poisson law,  $P_P(s) = \exp(-s)$ .

For  $\alpha < 1$ , the previous theories predict that all states should be delocalized, independently of the value of  $b$ . The inverse participation ratio (IPR) should then be proportional to the system size, as for Gaussian orthogonal ensembles (GOE), although higher order cumulants of the IPR should not necessarily behave in the same way as GOE [10]. For extended states, the nearest neighbor level spacing distribution approximately follows Wigner-Dyson law [14],  $P_{WD}(s) = (\pi s/2) \exp(-\pi s^2/4)$ .

At the critical value  $\alpha = 1$ , we expect to have multifractal eigenstates and critical level statistics, intermediate between Poisson and Wigner-Dyson. Recent numerical calculations at criticality and for  $b = 1$  have shown that the nearest level spacing distribution differs from the typical one at a metal-insulator transition [15].

Our aim in this paper is to explore in detail the characteristics of the PRBM model in the interesting regime around  $\alpha \approx 1$  and for the case  $b = 1$  where theoretical treatments are not strictly applicable. We do so by studying systematically the nearest level spacing distribution function  $P(s)$ , the behavior of the Green function (GF) as a function of distance, and the fractal properties of the states. We consider the PRBM Hamiltonian given by Eq. (1) with the exponent  $\alpha$  ranging between 0.3 and 2. In order to reduce edge effects, we use periodic boundary conditions, so that our systems are rings of length  $L$ . We have checked that the results do not differ significantly from those obtained for linear chains away from the ends.

We first calculate the eigenvalues of the Hamiltonian matrix by direct numerical diagonalization in order to study  $P(s)$ . We consider a small energy window  $(-0.4, 0.4)$  at the center of the band. For this calculation, the system size varies from  $L = 200$  to 5000, and the number of random realizations is equal to  $10^6/L$ . We quantitatively analyze the scaling behavior of  $P(s)$  through the following function of its variance [16,17]:

$$\eta(L, \alpha) = \frac{\text{var}(s) - 0.286}{1 - 0.286}, \quad (2)$$

which describes the relative deviation of  $\text{var}(s)$  from the Wigner-Dyson limit due to the finiteness of the system. In Eq. (2),  $\text{var}(s) = \langle s^2 \rangle - \langle s \rangle^2$ , and 0.286 and 1 are the

variances of Wigner-Dyson and Poisson distributions, respectively. We check that the use of other scaling variables [18,19], instead of  $\eta$ , do not alter the results.

Figure 1 shows the  $\alpha$  dependence of  $\eta$  for different system sizes:  $L = 200$  ( $\circ$ ),  $500$  ( $\triangle$ ),  $1000$  ( $\nabla$ ),  $3000$  ( $\square$ ), and  $5000$  ( $\diamond$ ). The value of  $\eta$  at  $\alpha = 1$  is independent of system size and very close to the GOE value, instead of being intermediate between Wigner-Dyson and Poisson such as in a standard metal-insulator transition. This is compatible with the numerical calculations of Ref. [15], where it was found that the spectral statistics at  $\alpha = 1$  differs from that typical of such a transition. For  $\alpha > 1$  there is a strong increase of  $\eta$  with both system size and  $\alpha$  towards the Poisson limit. For  $\alpha < 1$ ,  $\eta$  is basically independent of system size and very similar to the GOE value. The small value of  $\eta$  at criticality makes it difficult to decide whether there is a crossover at  $\alpha = 1$ , as in standard metal-insulator transitions. It also indicates that, for  $b = 1$ , the present transition is characterized by a very large conductance. This characteristic conductance would decrease with decreasing  $b$  [11].

Next, we calculate the real space GF  $G(i, j; E)$  as the inverse of the Hamiltonian matrix. For each value of  $\alpha$  and  $L$ , we obtain  $G(i, j; 0)$  at the center of the band  $E = 0$  for different disorder realizations. We first average with respect to the initial position and then we make an ensemble average of the logarithm of this quantity, obtaining

$$F(n) \equiv \left\langle \ln \sum_i |G(i, i+n; 0)| \right\rangle - \ln L. \quad (3)$$

In this case, the system size varies from  $L = 300$  to  $4000$ , and the number of random realizations is equal to  $10^6/L$ .

In Fig. 2 we plot  $F(n) - F(0)$  as a function of  $n$  for  $L = 4000$  and for different values of the exponent  $\alpha =$

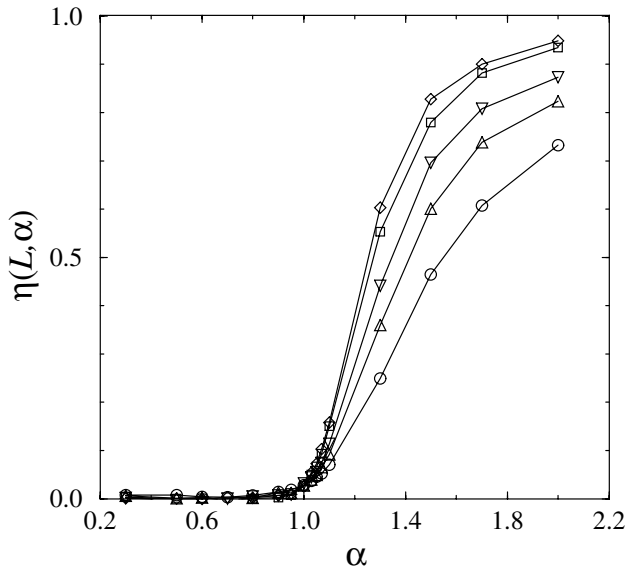


FIG. 1. Scaling variable  $\eta$  as a function of  $\alpha$  for different system sizes:  $L = 200$  ( $\circ$ ),  $500$  ( $\triangle$ ),  $1000$  ( $\nabla$ ),  $3000$  ( $\square$ ), and  $5000$  ( $\diamond$ ). Up to  $\alpha = 1$ ,  $\eta$  is basically independent of  $L$ .

0.7, 0.8, 0.85, 0.9, 0.95, and 1. We subtract  $F(0)$  in order to remove effects associated with variations in the average density of states. The central region (tail) of the results can be fitted very well by a sum of two power-law terms with the same exponent  $\beta$ :

$$F(n) - F(0) = \ln \left\{ \frac{A}{n^\beta} + \frac{A}{(L-n)^\beta} \right\}, \quad (4)$$

where  $A$  is a constant proportional to the density of states. Each contribution in Eq. (4) corresponds to propagation along one arm of the ring. The exponent  $\beta$  is closely related to the matrix exponent  $\alpha$  and weakly dependent on system size. The fit of Eq. (4) to the experimental points is so good that it is indistinguishable from the data on the scale used in Fig. 2. Up to the large scales used, states are not truly extended. The results for  $\alpha > 1$  (not shown) are similar to those represented in the figure, for  $\alpha \leq 1$ .

We have tried different extrapolation schemes in order to obtain the large scale behavior of the exponent  $\beta$ . We found that a logarithmic dependence on system size  $L$  fits fairly well the results, as can be seen in Fig. 3, where we plot  $\beta$  (solid symbols) versus  $L$  for  $\alpha = 0.8, 0.9, 0.95, 1, 1.05$ , and  $1.1$  on a semilogarithmic scale. The data can be fitted within errors by straight lines. The value of  $\beta$  for the critical case,  $\alpha = 1$ , is size independent and equal to 0.25. For  $\alpha < 1$ ,  $\beta$  decreases with size towards 0, while for  $\alpha > 1$  it increases towards  $\alpha$ . In the limit of macroscopic sizes, let us say,  $L \approx 10^8$ , we have a finite regime where the value of the exponent  $\beta$  is different from zero, and so states are not conducting. For infinitely large sizes  $\beta$  is zero below the transition, 0.25 at the transition, and  $\alpha$  above the transition.

To clarify the nature of the wave functions which give rise to this anomalous behavior of the GF, we calculate their fractal dimensions in the region around  $\alpha = 1$ . We

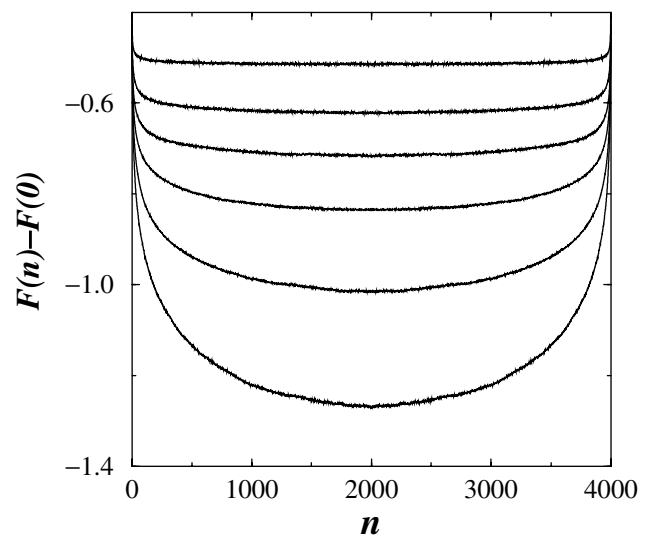


FIG. 2.  $F(n) - F(0)$  as a function of  $n$  for  $L = 4000$  and  $\alpha = 0.7, 0.8, 0.85, 0.9, 0.95$ , and  $1$ , from top to bottom.

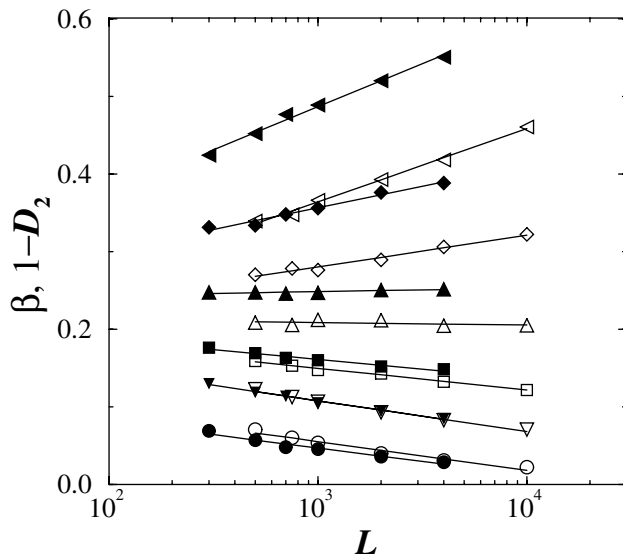


FIG. 3. Exponent  $\beta$  characterizing the decrease with distance of the GF (solid symbols) and one minus the fractal dimension  $1 - D_2$  (empty symbols) as a function of  $L$  on a logarithmic scale for  $\alpha = 0.8, 0.9, 0.95, 1, 1.05,$  and  $1.1$ , from bottom to top. Solid lines are linear fits to the data.

obtain the eigenfunctions of the Hamiltonian matrix by direct numerical diagonalization for system sizes ranging between  $L = 500$  and  $10\,000$ . For  $0.75 \lesssim \alpha \lesssim 1.25$ , we found that the wave functions show a complex structure with many sharp peaks of different heights and irregular spacing, which suggests the possibility of multifractal characteristics. We calculate the generalized fractal dimensions  $D_q$  by the standard box counting procedure through the expression

$$D_q = \frac{1}{q-1} \lim_{\delta \rightarrow 0} \frac{\ln[\chi_q(l)]}{\ln \delta}, \quad (5)$$

where  $\delta = l/L$ , and  $\chi_q(l)$  is the  $q$ th moment of the probability density of the wave function in the boxes of size of  $l$  [20]. For the evaluation of  $D_1$  from the previous equation, one has to expand  $\chi_q(l)$  around  $q = 1$ . In practice, we compute Eq. (5) at  $\delta = 0.1$ .

We concentrate on the correlation dimension  $D_2$ , which reflects the scaling of the density-density correlation function. We found that, as for the exponent  $\beta$ , a logarithmic dependence of  $D_2$  with  $L$  fits fairly well the numerical data. We also found the following empirical relation between  $\beta$  and  $D_2$ :

$$\beta + D_2 = \begin{cases} 1 & \text{for } \alpha < 1 \\ \alpha & \text{for } \alpha \geq 1. \end{cases} \quad (6)$$

To show graphically this relationship, we plot in Fig. 3, together with  $\beta$  (solid symbols), the value of  $1 - D_2$  (empty symbols) as a function of  $L$  for  $\alpha = 0.8, 0.9, 0.95, 1, 1.05,$  and  $1.1$ , from bottom to top. In agreement with Eq. (6), the data for  $\beta$  and  $1 - D_2$  overlap for  $\alpha < 1$ , while they are approximately shifted by an amount  $\alpha - 1$

for  $\alpha > 1$ . This shift is consistent with the fact that in this regime  $D_2$  tends towards zero, while  $\beta$  goes to  $\alpha$ .

At  $\alpha = 1$ ,  $D_2$  is practically size independent and equal to  $0.8$ . It very slowly tends to  $0$  for  $\alpha > 1$  and to  $1$  for  $\alpha < 1$ , but even for (finite) macroscopic sizes remains between  $0$  and  $1$  for a finite width interval of the parameter  $\alpha$ . The value of  $D_2/d$  at criticality is larger than for the standard Anderson metal-insulator transition in 3D [20],  $1.68/3 = 0.56$ , which indicates that the characteristic critical dimensionless conductance for the PRBM model with  $b = 1$  is larger than for the Anderson model. This is in agreement with the small value found for the variance of the nearest level spacing at criticality (Fig. 1).

As for  $D_2$ , the other fractal dimensions are size independent at criticality. We obtained that the information (or entropy) dimension  $D_1$  is equal to  $0.88$ . Other fractal dimensions are  $D_{-2} = 1.27$ ,  $D_{-1} = 1.14$ ,  $D_3 = 0.71$ , and  $D_4 = 0.65$ . Trivially the similarity dimension  $D_0 = d$ . In the range of dimensions studied, the deviations with respect to the weak multifractality limit, where  $(D_q/d) - 1 \propto q$ , are of the order of  $10\%$ .

Away from the critical point, the wave functions are fractal up to a given length, which depends drastically on  $\alpha$  and diverges as  $\alpha$  goes to unity. This length  $\xi_{\text{frac}}$  is defined as the system size for which the correlation dimension becomes either  $0$  or  $1$  in a plot such as Fig. 3. In Fig. 4 we show  $\log \xi_{\text{frac}}$  as a function of  $\alpha$ . We see that  $\log \xi_{\text{frac}}$  diverges at  $\alpha = 1$  in an asymmetric way, unlike in standard metal-insulator transitions. In the regime  $\alpha > 1$ , a perturbative treatment of the nonlinear  $\sigma$  model predicts the existence of a length scale  $\xi$ ,

$$\log \xi \sim c \frac{2\alpha - 1}{2\alpha - 2}, \quad (7)$$

which plays the role of the localization length for the PRBM model [10,11]. Note that  $\xi$  is not a length characterizing an exponential decay of the wave function, since

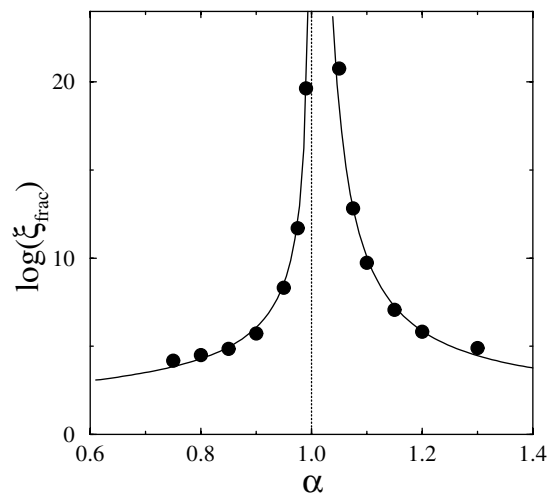


FIG. 4. Length  $\xi_{\text{frac}}$  as a function of  $\alpha$ . Solid lines correspond to Eq. (7) with  $c = 1.67$ , and Eq. (8) with  $c = 1.92$  and  $\nu = 0.5$ .

the GF, for system sizes larger than  $\xi_{\text{frac}}$ , decreases with distance as a power law with an exponent equal to  $\alpha$ . For this reason, it is the logarithm of  $\xi_{\text{frac}}$  rather than  $\xi_{\text{frac}}$  itself that diverges in Eq. (7) with a critical exponent and so plays the role of a localization length in a standard metal-insulator transition. Equation (7) was obtained for the regime  $b \gg 1$ , and the constant  $c$  was estimated to be of the order of  $\log b$ , although one can expect it to be qualitatively valid for any value of  $b$ . Our data in the localized regime can be fitted very well by a curve of the form given by Eq. (7), as can be seen in Fig. 4, where the right continuous curve corresponds to this equation with  $c = 1.67$ . This value of  $c$  is larger than predicted by the theory if extended to our case  $b = 1$ .

For  $\alpha < 1$ , the data of Fig. 4 cannot be fitted by Eq. (7), which corresponds to a critical exponent equal to unity, and there is no other theoretical prediction available. In this regime, the data can be fitted to a curve of the form

$$\log \xi \sim \frac{c}{|\alpha - 1|^\nu}, \quad (8)$$

with the critical exponent  $\nu$  equal to 0.5. The left solid line in Fig. 4 corresponds to Eq. (8) with  $\nu = 0.5$  and the fitting parameter  $c = 1.92$ . It is the first time to our knowledge that a metal-insulator transition is approached by two different critical exponents, which is in contradiction with a single parameter scaling theory. The possibility of the existence of two characteristic lengths has been already pointed out in a different one-dimensional model [21]. We note that we are able to obtain two exponents numerically because the transition point is known exactly ( $\alpha = 1$ ), which constitutes a key advantage of this model.

In summary, we have explored the critical region of the PRBM model in the case  $b = 1$  inaccessible to field theoretical methods. Our results, although compatible with theoretical predictions, shed new light on the specific form of the GF and on the multifractal structure of the wave functions near the critical point. The wave functions are fractal up to a given length which diverges asymmetrically with two different critical exponents at  $\alpha = 1$ . It is the first time that such an asymmetry has been obtained, in part due to the exact knowledge of the position of the critical point. The possibility of a similar asymmetric behavior in other metal-insulator transitions should be reconsidered. We note that a fitting procedure of the raw data without an exact knowledge of the critical value of the transition parameter is compatible with equal exponents in the di-

verging lengths, above and below the transition. The fractal behavior is correlated with a power-law decay of the GF with small exponents. The sum of the exponent characterizing the GF decay and the correlation dimension is approximately equal to unity in the localized phase and to  $\alpha$  in the extended phase. All this should have important consequences in the problem of two interacting particles and in the other problems related to the PRBM model, although their study is clearly outside the scope of this work.

We would like to thank the Spanish DGESIC, Projects No. BFM2000-1059 and No. 1FD97-1358, for financial support.

---

\*Present address: Department of Physics, California State University at Bakersfield, Bakersfield, CA.

- [1] A. D. Mirlin *et al.*, Phys. Rev. E **54**, 3221 (1996).
- [2] B. L. Altshuler and L. S. Levitov, Phys. Rep. **288**, 487 (1997).
- [3] I. V. Ponomarev and P. G. Silvestrov, Phys. Rev. B **56**, 3742 (1997).
- [4] G. Casati and T. Prosen, Physica (Amsterdam) **131D**, 293 (1999); F. Borgonovi *et al.*, Physica (Amsterdam) **131D**, 317 (1999).
- [5] V. E. Kravtsov, Ann. Phys. (Leipzig) **8**, 621 (1999).
- [6] V. E. Kravtsov and A. M. Tselvik, Phys. Rev. B **62**, 9888 (2000).
- [7] B. Grémaud and S. R. Jain, J. Phys. A **31**, L637 (1998).
- [8] E. B. Bogomolny, U. Gerland, and C. Schmit, Phys. Rev. E **59**, R1315 (1999).
- [9] G. Auberson, S. R. Jain, and A. Khare, J. Phys. A **34**, 695 (2001).
- [10] A. D. Mirlin, Phys. Rep. **326**, 259 (1999).
- [11] F. Evers and A. D. Mirlin, Phys. Rev. Lett. **84**, 3690 (2000).
- [12] L. Levitov, Europhys. Lett. **9**, 83 (1989); Phys. Rev. Lett. **64**, 547 (1990).
- [13] C. Yeung and Y. Oono, Europhys. Lett. **4**, 1061 (1987).
- [14] M. L. Mehta, *Random Matrices* (Academic Press, Boston, 1991).
- [15] I. Varga and D. Braun, Phys. Rev. B **61**, R11 859 (2000).
- [16] E. Cuevas, Phys. Rev. Lett. **83**, 140 (1999).
- [17] E. Cuevas, E. Louis, and J. A. Vergés, Phys. Rev. Lett. **77**, 1970 (1996).
- [18] J. Pipek and I. Varga, Phys. Rev. A **46**, 3148 (1992).
- [19] B. I. Shklovskii *et al.*, Phys. Rev. B **47**, 11 487 (1993).
- [20] M. Schreiber and H. Grussbach, Phys. Rev. Lett. **67**, 607 (1991).
- [21] Lev I. Deych, A. A. Lisyansky, and B. L. Altshuler, Phys. Rev. Lett. **84**, 2678 (2000).